Abstract. STIS Echelle observations at a resolution of $10\,\mathrm{km\,s^{-1}}$ and UVES/VLT spectroscopy at a resolution of $7\,\mathrm{km\,s^{-1}}$ of the luminous QSO HE 0515-4414 ($z_{\mathrm{em}} = 1.73$, $B = 15.0$) reveal four intervening O VI absorption systems in the redshift range $1.21 \leq z_{\mathrm{abs}} \leq 1.67$ (1.38503, 1.41601, 1.60175, 1.67359). In addition two associated systems at $z = 1.69707$ and $z = 1.73585$ are present. Noteworthy is an absorber at $z = 1.385$ with $\log N_{\mathrm{H\,I}} = 13.9$ and strong O VI (N(O VI)/N(H I) ≈ 1) and C IV doublets, while a nearby much stronger Ly α absorber ($\log N_{\mathrm{H\,I}} = 14.8$, $\Delta v = 123\,\mathrm{km\,s^{-1}}$) does not reveal any heavy element absorption. For the first time high resolution observations allow to measure radial velocities of H I, C IV and O VI simultaneously in several absorption systems (1.385, 1.674, 1.697) with the result that significant velocity differences (up to $18\,\mathrm{km\,s^{-1}}$) are observed between H I and O VI, while smaller differences (up to $5\,\mathrm{km\,s^{-1}}$) are seen between C IV and O VI. We tentatively conclude that H I, O VI, and C IV are not formed in the same volumes and that therefore implications on ionization mechanisms are not possible from observed column density ratios O VI/H I or O VI/C IV. The number density of O VI absorbers with $W_{\mathrm{rest}} \geq 25\,\mathrm{m\AA}$ is $\mathrm{d}N/\mathrm{d}z \leq 10$, roughly a factor of 5 less than what has been found by Tripp at al. (2000) at low redshift. However, this number is uncertain and further lines of sight will be probed in the next HST cycle. An estimate of the cosmological mass-density of the O VI-phase yields $\Omega_{\mathrm{b}}(\mathrm{O\,VI}) \approx 0.0003\,h_{75}^{-1}$ for $[\mathrm{O/H}] = -1$ and an assumed ionization fraction O VI/O $= 0.2$. It should be noted that this result is subject to large systematic errors. This corresponds to an increase by roughly a factor of 15 between $\bar{z} = 1.5$ (this work) and the value found by Tripp et al. (2000) at $\bar{z} = 0.21$, if the same oxygen abundance $[\mathrm{O/H}] = -1$ is assumed. Agreement with the simulations by Davé et al. (2001) can be obtained, if the oxygen abundance increases by a factor of ~ 3 over the same redshift interval.

Key words: cosmology: observations – intergalactic medium – quasars: absorption lines – quasars: individual: HE 0515-4414

A&A manuscript no.
(will be inserted by hand later)

Your thesaurus codes are:
missing; you have not inserted them

ASTRONOMY AND ASTROPHYSICS

High-resolution O VI absorption line observations at $1.2 \leq z \leq 1.7$ in the bright QSO HE 0515-4414 *

Dieter Reimers[1], Robert Baade[1], Hans-Jürgen Hagen[1], and Sebastian Lopez[2]

[1] Hamburger Sternwarte, Universität Hamburg, Gojenbergsweg 112, D-21029 Hamburg, Germany
email: dreimers@hs.uni-hamburg.de, rbaade@hs.uni-hamburg.de, hhagen@hs.uni-hamburg.de

[2] Departamento de Astronomia, Universidad de Chile, Casilla 36-D, Santiago, Chile
email: slopez@rhea.das.uchile.cl

received date; accepted date

1. Introduction

Recent observations of intervening O VI absorbers in HST-STIS Echelle spectra of bright, low redshift QSOs have provided strong evidence that in the local universe a considerable fraction of baryonic matter might be "hidden" in a warm ($\sim 10^5$ K) intergalactic medium (Savage et al. 1998; Tripp et al. 2000; Tripp & Savage 2000). This observation is in accordance with models of hierarchical structure formation by Cen & Ostriker (1999) and Davé et al. (2001) which predict that a considerable fraction of all baryons reside in a warm-hot phase of the intergalactic medium (WHIM) shock-heated to temperatures of $10^5 - 10^7$ K. The same models predict that the fraction of baryons residing in this WHIM increases strongly with decreasing redshift from less than 5 % at $z = 3$ to $30 - 40$ % at $z = 0$. Can this prediction be verified or disproved by observations, or can observations even impose constraints on the models? This appears difficult for various reasons. First of all, the WHIM is difficult to detect (cf. Davé et al. 2001), both as diffuse X-ray emission of the hotter parts or in absorption through the O VI doublet. In addition the temperature distribution of the WHIM varies with redshift so that a complete census would require the detection of all components as a function of redshift. The warm O VI component has the additional complication that both the oxygen abundance and the ionization process cannot be determined from O VI observations alone. While at low redshift ($z < 0.3$) collisional ionization is the most probable process since the ionizing extragalactic UV background is diluted, O VI can be produced easily by photoionization at redshifts ≥ 2 and has been observed to be ubiquitous in the low-density IGM (Schaye et al. 2000). On the other hand O VI is not expected to be produced by photoionization for $z \geq 3$ since the reionization of He II is incomplete (Reimers et al. 1997; Heap et al. 2000) and the IGM therefore opaque to photons with energies above 8.4 Rydberg. Remains the intermediate redshift range which for $z < 1.9$ requires high-resolution UV-spectroscopy of a bright, high-redshift QSO. In this paper, we present combined high-resolution HST/STIS observations of O VI absorption supplemented by ESO-VLT/UVES spectroscopy of the accompanying H I and C IV lines in the brightest known intermediate redshift QSO HE 0515-4414 ($z_{\mathrm{em}} = 1.73$, $B = 15.0$) discovered by the Hamburg/ESO Survey (Reimers et al. 1998). The data have been taken mainly with the aim to study the evolution of the Ly α forest and its metal content in the range $z = 1$ to 1.7. In this first paper we concentrate on intervening O VI absorption.

2. Observations and data reduction

2.1. Hubble Space Telescope observations

HE 0515-4414 was observed with STIS for 31 500 s in three visits between January 31 and February 2, 2000 with the medium resolution NUV echelle mode (E230M) and a 0.2×0.2 aperture which provides a resolution of $\sim 30\,000$ (FWHM $\simeq 10\,\mathrm{km\,s^{-1}}$). We used the HST pipeline data with an additional correction for inter-order background correction (Rosa, private communication). The spectrum covers the range between 2279 Å and ~ 3080 Å. The coverage at the red end guarantees overlap with the UVES spectra which extend shortwards to ~ 3050 Å.

2.2. VLT/UVES spectroscopy

Echelle spectra of HE 0515−4414 were obtained during commissioning of UVES at the VLT/Kueyen telescope. The observations were carried out under good seeing conditions (0.5 – 0.8 arcsec) and a slit width of 0.8 arcsec was used. A summary of the observations and

Send offprint requests to: D. Reimers

* Based on observations with the NASA/ESA Hubble Space Telescope, obtained at the Space Telescope Science Institute, which is operated by Aura, Inc., under NASA contract NAS 5-26555; and on observations collected at the VLT/Kueyen telescope, ESO, Paranal, Chile.

of the detectors used is given in the ESO web pages `http://www.hq.eso.org/instruments/uves`.

The spectra were extracted using an algorithm that attempts to reduce the statistical noise to a minimum. After bias-subtracting and flat-fielding of the individual CCD frames, the seeing profiles were fitted with a Gaussian in two steps. In a first step the three parameters of the Gaussian – width, amplitude, and offset from the previously defined orders – were unconstrained; in the second step only the amplitudes were allowed to vary, with width and offset held fixed at values found by a $\kappa\sigma$-clipping fit along the dispersion direction to the values obtained in the first step. Flux values were assigned with a variance according to the Poisson statistics and the read-out noise, while cosmic-ray shots were assigned with infinite variances. Thus, the extraction procedure recovers the total count number even at wavelengths where the spatial profile is partially modified by cosmic-ray hits.

The extracted spectra were wavelength calibrated using as reference Th-Ar spectra taken after each science exposure. All wavelength solutions were accurate to better than typically 1/10 pixel. The wavelength values were converted to vacuum heliocentric values and each spectrum of a given instrumental configuration was binned onto a common linear wavelength scale (of typically 0.04 Å per pixel). Finally, the reduced spectra were added weighting by the inverse of the flux variances.

2.3. Line profile analysis

Our analysis was carried out using a multiple line fit procedure to determine the parameters λ_c (line center wavelength), N (column density), and b (line broadening velocity) for each absorption component. We have written a FORTRAN program based on the Levenberg-Marquardt algorithm to solve this nonlinear regression problem (see, e.g., Bevington & Robinson 1992). We have included additional parameters describing the local continuum curvature by a low order Legendre polynomial. A free floating continuum is a prerequisite for an adequate profile decomposition in the case of complex line ensembles.

To improve the numerical efficiency we have to provide adequate initial parameters. In some cases the success of the fitting depends on good starting parameters, since the algorithm tends to converge to the nearest, not necessarily global, minimum of the chi-square merit function. A first approximation can be found neglecting the instrumental profile and converting the flux profile into apparent optical depths using the relation

$$\tau_a(\lambda) = \ln[F_c(\lambda)/F_{obs}(\lambda)]\,, \tag{1}$$

where F_c and F_{obs} are the continuum level and the observed line flux, respectively. If the instrumental resolution is high compared to the line width, $\tau_a(\lambda)$ will be a good representation of the true optical depth $\tau(\lambda)$. However, an ill-defined continuum level or saturation effects may produce large uncertainties. The apparent optical depth can be automatically fitted with a sum of Gaussians, each having a variable position, amplitude, and width. An a priori line identification is not necessary at this stage of the analysis.

Having obtained first-guess parameters we proceed with Doppler profile fitting using artificial test lines with $z = 0$ and $f = 1$, where f is the oscillator strength. It can be shown that most Voigt profiles are well represented by the purely velocity broadened Doppler core. The size of the fit region depends on the complexity and extent of the absorption line ensembles. Indeed, the number of free parameters should be less than 100 to preserve the numerical efficiency. One specific characteristic of our technique is the simultaneous continuum normalization which can reconstruct the true continuum level even in cases, where the background is hidden by numerous lines. The multi component profile is the convolution of the intrinsic spectrum and the instrumental spread function $P(\Delta\lambda)$:

$$F(\lambda) = P(\Delta\lambda) \otimes \left\{ F_c(\lambda) \prod_i \exp[-\tau_i(\lambda, \lambda_c, N, b)] \right\}\,. \tag{2}$$

If the program fails to converge on a reasonable model, the parameters can be adjusted by hand. In this way the fit can be modified to be acceptable by eye and then reminimized. In some exceptional cases this procedure is the only chance to free a converged solution from a local chi-square minimum.

After line identification the parameters of the test lines can be transformed to the actual redshift and oscillator strength. However, the contribution of unknown profile components can still be considered using the test line results. A final Voigt profile fit with all identified components includes the simultaneous multiplet treatment, keeping the redshift, column density, and line width the same during the chi-square minimization. The upper limit of the column densities of non-detected lines is estimated assuming a $5\,\sigma$ significance level for the equivalent width.

3. Absorption systems with O VI lines

We searched for O VI lines associated with known Ly α and Ly β absorbers. Therefore, as a starting point, we tried to identify all Ly α lines. Line identification and the analysis of the Ly α forest will be presented in some detail in a later paper. At the resolution of $\sim 30\,000$ (STIS) and $\sim 50\,000$ (UVES), narrow metal lines can usually be distinguished easily from hydrogen lines. In all Ly α absorption systems with column densities $\log N_H \geq 13.5$ we searched for metal lines, in particular for O VI, C IV, N V, Si IV, C III, N III. In a first step, all lines within $\pm 200\,\mathrm{km\,s^{-1}}$ were considered to be plausibly associated with the Ly α/Ly β systems. Within this selection criterium we have found 6 systems with probable O VI absorption, listed in Table 1. Due to the moderate S/N ratio of the STIS spectra (between 10 and 20 per resolution element) the detection limit of O VI is estimated to lie between $\log N = 13.3$ at the lower limit of the z range and $\log N = 13.1$ near the quasar.

– $z = 1.385$: The single O VI line and the C IV doublet correspond to the unsaturated Ly α line at 2899.42 Å. Both O VI and C IV are slightly blueshifted (by $-14\,\mathrm{km\,s^{-1}}$ and $-17\,\mathrm{km\,s^{-1}}$, respectively) relative to Ly α and Ly β (Fig. 1). The Doppler parameter of the C IV doublet of $8.2\,\mathrm{km\,s^{-1}}$ is determined reliably with the high-resolution, high S/N UVES spectra, while O VI, less certain, yields $13.5\,\mathrm{km\,s^{-1}}$. The absorbing cloud at z = 1.385 is a close neighbour to a strong Ly α/Ly β system at z = 1.386 ($+123\,\mathrm{km\,s^{-1}}$, $\log N_{\mathrm{H}} = 15.1$) with no heavy element absorption at all. The $z = 1.385$ system appears to represent the extremely rare case of a highly ionized cloud with low neutral hydrogen density ($\log N_{\mathrm{H}} = 13.9$). According to the velocity centroids, C IV and O VI are apparently not formed in the same volume. In addition, the velocity shift between H I and C IV/O VI is in favour of different phases (volumes). This behaviour is similar to what Tripp et al. (2000) have found in a system at z = 0.22637 in H 1821+643. Because apparently H I, C IV, and O VI are not formed in the same volume, there are no empirical constraints on the ionization mechanism (photoionization versus collisional ionization).

– $z = 1.416$: The absorber is seen in Ly α, Ly β and O VI 1031, while the O VI 1037 line is blended with Ly ε of a strong system at $z = 1.674$. Since again a velocity shift of $+22\,\mathrm{km\,s^{-1}}$ is seen between O VI 1031 and Ly α/Ly β, this system can only be considered as marginal.

– $z = 1.602$: Besides Ly α and Ly β, only the O VI doublet is detected at a velocity of $+18\,\mathrm{km\,s^{-1}}$ relative to the hydrogen main component. Notice that in velocity space the O VI doublet is located between two Ly α clouds (cf. Table 1, Fig. 1).

– $z = 1.674$: This absorbtion system is seen in Ly α down to Ly ε and exhibits a strong O VI doublet. The C IV doublet in our UVES spectra show that it consists of two components, a narrow ($b \simeq 9\,\mathrm{km\,s^{-1}}$), stronger component redshifted by $4.3\,\mathrm{km\,s^{-1}}$ relative to hydrogen, and a broad ($b \simeq 18\,\mathrm{km\,s^{-1}}$) component at $-12.8\,\mathrm{km\,s^{-1}}$. Noteworthy are the broad wings of Ly α which can be explained only with an additional extremely broad ($b > 100\,\mathrm{km\,s^{-1}}$) unsaturated ($\log N_{\mathrm{H}} = 14.1$) component which in velocity nearly coincides with the O VI line and the saturated Ly α Doppler core ($\log N_{\mathrm{H}} = 15.1$). The broad wing is not seen clearly in the other Lyman lines, but is still consistent with the lower S/N STIS spectra. This extremely broad component is probably caused by collapsing or expanding structures in the intergalactic medium.

– $z = 1.697$: This is a system with O VI, C IV, and N V doublets as well as C III 977 Å in combination with an unsaturated Ly α line. The high resolution UVES profiles of both C IV and N V show two components (Fig. 1): a strong one, nearly unshifted relative to hydrogen, and a weak one at $\sim -33\,\mathrm{km\,s^{-1}}$. The O VI 1037 Å line is at $+0.4\,\mathrm{km\,s^{-1}}$ with a possible second component at $-32.9\,\mathrm{km\,s^{-1}}$ (O VI 1031 Å is blended with a strong Ly α line at $z = 1.2897$). It seems a likely supposition that O VI is being formed in the same volume as C IV and N V. If so, the column density ratios O VI/C IV and O VI/N V as well as the high O VI/H I ratio are in favour of photoionization in the proximity zone of the QSO. Notice that HE 0515-4414 is one of the most luminous QSOs in the universe.

– $z = 1.736$: This is an associated system close to the systemic QSO redshift ($z_{\mathrm{em}} = 1.73$) which shows only the O VI doublet. Both C IV and N V are not detected, in spite of the high S/N of the UVES spectra. Again, the inferred lower limits to the column density ratios O VI/C IV and O VI/N V are consistent only with photoionization.

4. The cosmological mass-density of the O VI phase

With the present STIS spectra of HE 0515-4414 the redshift range $1.21 \leq z \leq 1.73$ has been covered for the first time at sufficiently high resolution to undertake a sensitive search for O VI absorbers. We have detected 6 O VI systems. Two of them (z = 1.697, 1.736) are either associated with the QSO or in the proximity zone of the extremely luminous QSO. The system $z = 1.416$ is marginal, since only the 1031 Å line is detected. Including the latter, we have 4 detections in the range z = 1.21 to 1.67 which yield a number density of O VI absorbers with $W_{\mathrm{rest}} \geq 25\,\mathrm{m\AA}$ of $\mathrm{d}N/\mathrm{d}z \leq 10$. Compared with the findings by Tripp et al. (2000) of $\mathrm{d}N/\mathrm{d}z = 48$ at $\bar{z} \simeq 0.21$, the number density at $\bar{z} \simeq 1.44$ is roughly a factor of 5 lower. Tripp et al. (2000) compared their finding of a high number density of weak O VI absorbers ($W_{\mathrm{rest}} \geq 30$ mÅ) in H 1821+643 and PG 0953+415 with other classes of absorbers and found that the weak O VI number density is more comparable to that of the low z weak Ly α absorbers – which have $\mathrm{d}N/\mathrm{d}z \approx 100$ for $W_{\mathrm{rest}} \geq 50\,\mathrm{m\AA}$ – than to other types of metal absorbers like Mg II. In HE 0515-4414 we have at least 42 Ly α systems (the exact number being unknown due to the line blending problem) with $W_{\mathrm{rest}} \geq 50\,\mathrm{m\AA}$ in the range $1.21 \leq z \leq 1.67$ which yields roughly $\mathrm{d}N/\mathrm{d}z = 90$ [1]. Among these, roughly half of them are strong, saturated Ly α lines with a detected Ly β line. Again, while our STIS spectrum of HE 0515-4414 con-

[1] A more detailed discussion of the Ly α forest in HE 0515-4414 is in progress

firms the number density of Ly α absorbers found previously (see Weymann et al. 1998), the number of O VI absorbers with $W_{\rm rest} \geq 25\,{\rm m\AA}$ is lower than the number of Ly α absorbers with $W_{\rm rest} \geq 50\,{\rm m\AA}$ by a factor of 10. It is noteworthy that, except the $z = 1.674$ system, O VI is detected in lower column density Ly α absorbers ($\log N_{\rm H} \leq 14$). Following the calculations by Tripp et al. (2000) and earlier work by Storrie-Lombardi et al. (1996) and Burles & Tytler (1996), the mean cosmological mass-density of O VI absorbers can be written in units of the critical density $\rho_{\rm c}$ as

$$\Omega_{\rm b}(\mathrm{O\,VI}) = \frac{\mu\, m_{\rm H}\, H_0}{\rho_{\rm c}\, c\, f(\mathrm{O\,VI})} \left(\frac{\rm O}{\rm H}\right)^{-1}_{\rm O\,VI} \frac{\sum_i N_i(\mathrm{O\,VI})}{\Delta X}, \quad (3)$$

where [O/H] is the assumed oxygen abundance in the O VI absorbing gas, $f(\mathrm{O\,VI})$ is the fraction of oxygen in O VI, $\sum_i N_i(\mathrm{O\,VI})$ is the total O VI column density from all absorbers, and ΔX is the absorption distance (Bahcall & Peebles 1969).

Over the redshift interval $z = 1.21$ to $z = 1.67$ we have $\Delta X = 0.72$ for $q_0 = 1/2$. $\sum_i N_i(\mathrm{O\,VI})$ is $2.1 \times 10^{14}\,{\rm cm}^{-2}$ (Table 1). Assuming $f(\mathrm{O\,VI}) = 0.2$, following Tripp et al. (2000) and Tripp & Savage (2000), which is close to the maximum for both collisional ionization and photoionization, we obtain a lower limit $\Omega_{\rm b}(\mathrm{O\,VI}) \geq 3 \times 10^{-5}\ [({\rm O/H})/({\rm O/H})_\odot]^{-1}\, h_{75}^{-1}$. The only reliably measured heavy element abundances at $\bar{z} = 1.4$ are from DLAs. Typically the metal abundance (e.g. from Zn) is 1/10 solar (Pettini et al. 1999, Vladilo et al. 2000). There is, however, no guarantee that these abundances apply also to the O VI absorbers among the low column density systems. Assuming 1/10 solar for the oxygen abundance, we have $\Omega_{\rm b}(\mathrm{O\,VI}) \geq 3\times10^{-4}\, h_{75}^{-1}$. With the same assumptions Tripp et al. (2000) derived a value $\geq 4 \times 10^{-3}\, h_{75}^{-1}$. Using a somewhat different formalism for the derivation of $\Omega_b(\mathrm{O\,VI})$, namely Eq. (6) from Tripp & Savage (2000), we get with the same assumptions $\Omega_{\rm b}(\mathrm{O\,VI}) \geq 1.5\times10^{-4}\, h_{75}^{-1}$. Both from the number counts of the O VI systems and the estimate of the mean O VI density the unavoidable conclusion seems to be that at $\bar{z} = 1.5$, the baryon content of the O VI phase contains a factor of ≥ 10 less material than at $\bar{z} = 0.21$.

5. Conclusions

Our results on O VI absorbing clouds in HE 0515-4414 can be summarized as follows:

- Intervening O VI systems per unit redshift appear to be less frequent by a factor of ~ 5 at $\bar{z} = 1.5$ compared to the local universe $\bar{z} = 0.21$.
- According to the observed velocities, the O VI lines are not formed in the same volume as the H I and C IV absorbing material. This conclusion is supported by the derived Doppler parameters (see Table 1). An identical gas phase would require $b_{\rm O\,VI} \leq b_{\rm C\,IV}$ in contradiction to the observations.
- Consequently, even narrow related C IV lines which would eliminate collisional ionization as mechanism for C IV production, cannot rule out collisional ionization for O VI from observations. For the same reason, O VI/C IV column density ratios cannot be used for arguing in favour of or against photoionization/collisional ionization.

The occurrence of an extremely broad component superimposed on the "normal" Doppler profile as observed in the $z = 1.674$ system is a rare Ly α profile type. In fact, we have never seen such a profile combination. In the context of modern interpretations of the Ly α forest as caused by a gradually varying density field characterized by a network of filaments and sheets (e.g. Bi & Davidsen), a multi-component Voigt profile fitting is artificial and without a physical meaning anyway. The observed Ly α profile at $z = 1.674$ could be easily modelled by an overdense structure with inflow or outflow velocities of the order of $100\,{\rm km\,s^{-1}}$. We abstain from such an exercise, since the line profile decomposition would not lead to a unique solution. Remarkable is the coincidence with a strong O VI doublet at the same velocity.

Our finding, that the O VI phase at $\bar{z} = 1.5$ contains a factor of ≥ 10 less material than at z = 0.21, provided the O VI/O ratio and the oxygen abundance are similar, appears to be inconsistent with the simulations of Davé et al. (2001) who predict an increase of the mass-fraction of baryons in the warm-hot phase of the IGM by at most a factor of 4 between $z = 1.5$ and 0.2. An increase in the mean oxygen abundance in the low density IGM by a factor of ~ 3 over the same redshift range would restore consistency with the theoretical predictions. However, at present we do not see a possibility to test this hypothesis. Furthermore, as long as we do not understand the ionization to O VI quantitatively, the fractional ionization O VI/O might vary between $z = 1.5$ and 0.2. Finally, our result is still debatable due to small number statistics. More lines of sight, both at low and intermediate redshift, have to be probed.

Acknowledgements. This work has been supported by the Verbundforschung of the BMBF/DLR under Grant No. 50 OR 99111. S.L. acknowledges financial support by FONDECYT grant N°3 000 001 and by the Deutsche Zentralstelle für Arbeitsvermittlung.

References

Bahcall J.N., Peebles P.J. E., 1969, ApJ 156, L7
Bevington P.R., Robinson D.K., 1992, Data Reduction and Error Analysis for the Physical Sciences, McGraw-Hill, New York
Bi H., Davidsen A.F., 1997, ApJ 479, 523
Burles S., Tytler D., 1996, ApJ 460, 584
Cen R., Ostriker J.P., 1999, ApJ 519, L109
Davé R., Cen R., Ostriker J.P. et al., 2001, ApJ 552, 473
Heap S., Williger G.M., Smette A. et al., 2000, ApJ 534, 69

Pettini M., Ellison S.L., Steidel C.L., Bowen D.V., 1999, ApJ 510, 576
Reimers D., Köhler S., Wisotzki L. et al., 1997, A&A 327, 890
Reimers D., Hagen H.-J., Rodriguez-Pascual P., Wisotzki L., 1998, A & A 334, 96
Savage B.D., Tripp T.M., Lu L., 1998, AJ 115, 436
Schaye J., Rauch M., Sargent W.L.W., Kim T.-S., 2000, ApJ 541, L1
Storrie-Lombardi L.J., McMahon R.G., Irwin M.J., 1996, MNRAS 283, L79
Tripp T.M., Savage B.D., 2000, ApJ 542, 42
Tripp T.M., Savage B.D. Jenkins E.B., 2000, ApJ 534, L1
Vladilo G., Bonifacio P., Centurion M., Molaro P., 2000, ApJ 543, 24
Weymann R., Januzzi B.T., Lu L. et al., 1998, ApJ 506, 1

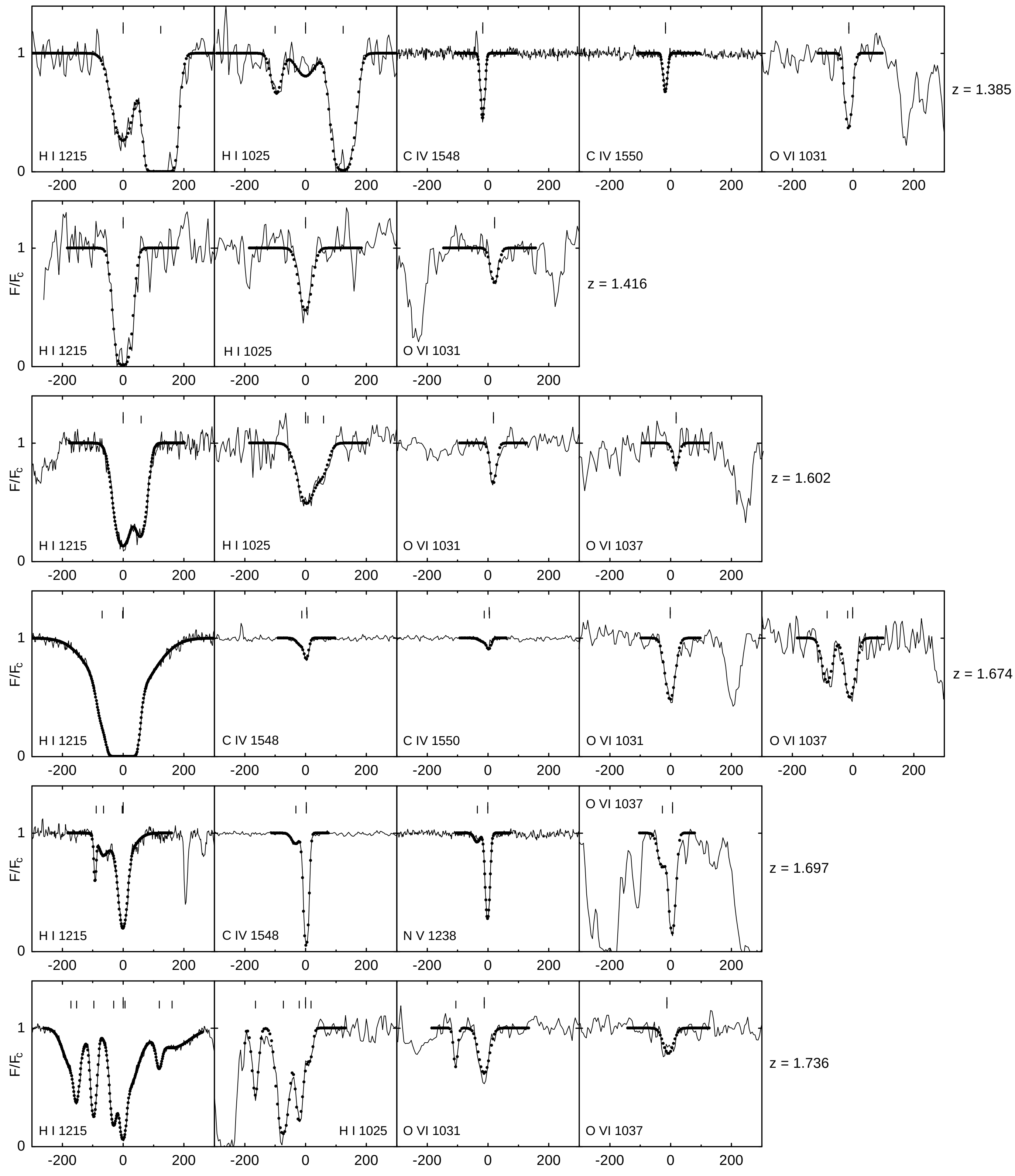

Fig. 1. Selected absorption line profiles of systems with O VI detection. The normalized flux is plotted vs. rest-frame velocity of the hydrogen main component. Long tick marks indicate the position of the primary lines, while short tick marks indicate additional absorption components. It should be noted that some profile ensembles contain lines which do not belong to the same absorption system. The dotted curves represent our fit models

Table 1. Absorption line systems with O VI detections

Ion	λ_0 (Å)	$\lambda_{\rm obs}$ (Å)	z	log N	b (km s^{-1})	$W_{\rm rest}$ (mÅ)	Δv (km s^{-1})
z=1.385							
H I	1025.722	2446.383	1.385035 ± 0.000019	13.86 ± 0.03	40.6 ± 3.5	50	0.0
	1025.722	2447.391	1.386017 ± 0.000008	15.10 ± 0.07	32.8 ± 1.3	309	+123.4
	1215.670	2899.415	1.385035 ± 0.000019	13.86 ± 0.03	10.6 ± 3.5	258	0.0
	1215.670	2900.609	1.386017 ± 0.000008	15.10 ± 0.07	32.8 ± 1.3	517	+123.4
C III	977.020	2330.005	1.384808 ± 0.000031	12.76 ± 0.22	7.4 ± 7.0	28	−28.5
C IV	1548.195	3692.288	1.384899 ± 0.000001	13.21 ± 0.01	8.2 ± 0.2	47	−17.1
	1550.770	3698.429	1.384899 ± 0.000001	13.21 ± 0.01	8.2 ± 0.2	27	−17.1
Si IV				< 12.0			
N V				< 12.8			
O VI	1031.926	2461.064	1.384923 ± 0.000012	13.88 ± 0.06	13.5 ± 2.2	65	−14.1
	1037.617	blend					
z=1.416							
H I	1025.722	2478.159	1.416014 ± 0.000011	14.21 ± 0.05	25.6 ± 1.6	94	0.0
	1215.670	2937.075	1.416014 ± 0.000011	14.21 ± 0.05	25.6 ± 1.6	290	0.0
C III	977.020	blend					
C IV				< 11.9			
Si IV				< 11.6			
N V				< 13.3			
O VI	1031.926	2493.327	1.416188 ± 0.000027	13.43 ± 0.12	14.5 ± 5.2	30	+21.6
	1037.617	blend					
z=1.602							
H I	1025.722	2668.702	1.601779 ± 0.000016	13.95 ± 0.03	32.8 ± 1.9	59	0.0
	1025.722	2669.193	1.602288 ± 0.000016	13.68 ± 0.04	24.1 ± 1.8	32	+58.6
	1215.670	3162.905	1.601779 ± 0.000016	13.95 ± 0.03	32.8 ± 1.9	251	0.0
	1215.670	3163.523	1.602288 ± 0.000016	13.68 ± 0.04	24.1 ± 1.8	155	+58.6
C III				< 12.4			
C IV				< 11.8			
Si IV				< 11.7			
N V				< 12.5			
O VI	1031.926	2685.006	1.601937 ± 0.000017	13.46 ± 0.07	12.5 ± 3.6	31	+18.2
	1037.617	2699.813	1.601937 ± 0.000017	13.46 ± 0.07	12.5 ± 3.6	16	+18.2
z=1.674							
H I	949.743	2539.247	1.673615 ± 0.000015	14.07 ± 0.02	112.7 ± 3.8	13	−1.4
	949.743	2539.259	1.673628 ± 0.000007	15.07 ± 0.03	30.9 ± 0.7	103	0.0
	972.537	2600.189	1.673615 ± 0.000015	14.07 ± 0.02	112.7 ± 3.8	27	−1.4
	972.537	2600.201	1.673628 ± 0.000007	15.07 ± 0.03	30.9 ± 0.7	173	0.0
	1025.722	2742.386	1.673615 ± 0.000015	14.07 ± 0.02	112.7 ± 3.8	82	−1.4
	1025.722	2742.399	1.673628 ± 0.000007	15.07 ± 0.03	30.9 ± 0.7	292	0.0
	1215.670	3250.234	1.673615 ± 0.000015	14.07 ± 0.02	112.7 ± 3.8	466	−1.4
	1215.670	3250.249	1.673628 ± 0.000007	15.07 ± 0.03	30.9 ± 0.7	466	0.0
C III	977.020	blend					
C IV	1548.195	4139.120	1.673514 ± 0.000112	12.45 ± 0.37	18.3 ± 10.1	10	−12.8
	1548.195	4139.356	1.673666 ± 0.000009	12.59 ± 0.25	9.1 ± 2.3	14	+4.3
	1550.770	4146.005	1.673514 ± 0.000109	12.45 ± 0.37	18.3 ± 10.1	5	−12.8
	1550.770	4146.241	1.673666 ± 0.000010	12.59 ± 0.25	9.1 ± 2.3	7	+4.3
Si IV				< 11.6			
N V				< 12.2			
O VI	1031.926	2758.972	1.673614 ± 0.000013	13.88 ± 0.04	20.2 ± 2.0	74	−1.2
	1037.617	2774.187	1.673614 ± 0.000013	13.88 ± 0.04	20.2 ± 2.0	42	−1.2

Table 1. Continued

Ion	λ_0 (Å)	$\lambda_{\rm obs}$ (Å)	z	log N	b (km s^{-1})	$W_{\rm rest}$ (mÅ)	Δv (km s^{-1})
<u>z=1.697</u>							
H I	1025.722	blend					
	1215.670	3278.803	1.697116 ± 0.000003	13.48 ± 0.03	15.9 ± 0.7	100	0.0
C III	977.020	2635.121	1.697101 ± 0.000013	12.96 ± 0.08	8.5 ± 2.3	40	−1.7
C IV	1548.195	4175.207	1.696822 ± 0.000011	12.61 ± 0.04	18.6 ± 2.0	18	−32.7
	1548.195	4175.682	1.697129 ± 0.000001	13.82 ± 0.01	8.4 ± 0.1	122	+1.5
	1550.770	4182.151	1.696822 ± 0.000011	12.61 ± 0.04	18.6 ± 2.0	9	−32.7
	1550.770	4182.627	1.697129 ± 0.000001	13.82 ± 0.01	8.4 ± 0.1	89	+1.5
Si IV	1393.755	3759.174	1.697156 ± 0.000016	11.56 ± 0.09	8.5*	3	+4.4
	1402.770	3783.489	1.697156 ± 0.000016	11.56 ± 0.09	8.5*	2	+4.4
N V	1238.821	3340.882	1.696824 ± 0.000022	12.47 ± 0.13	10.7 ± 3.9	6	−32.5
	1238.821	3341.236	1.697109 ± 0.000002	13.61 ± 0.01	8.4 ± 0.3	53	−0.8
	1242.804	3351.623	1.696824 ± 0.000022	12.47 ± 0.13	10.7 ± 3.9	3	−32.5
	1242.804	3351.978	1.697109 ± 0.000002	13.61 ± 0.01	8.4 ± 0.3	33	−0.8
O VI	1031.926	2782.919	1.696820 ± 0.000029	13.77 ± 0.09	16.7 ± 4.0	58	−32.9
	1031.926	2783.229	1.697120 ± 0.000008	14.40 ± 0.04	11.8 ± 1.3	112	+0.4
	1037.617	2798.266	1.696820 ± 0.000029	13.77 ± 0.09	16.7 ± 4.0	33	−32.9
	1037.617	2798.577	1.697120 ± 0.000008	14.40 ± 0.04	11.8 ± 1.3	85	+0.4
<u>z=1.736</u>							
H I	1025.722	2806.274	1.735901 ± 0.000003	13.50 ± 0.02	10.9 ± 0.5	21	0.0
	1215.670	3325.952	1.735901 ± 0.000003	13.50 ± 0.02	10.9 ± 0.5	86	0.0
C III				< 12.4			
C IV				< 11.7			
Si IV				< 11.6			
N V				< 12.3			
O VI	1031.926	2823.133	1.735790 ± 0.000017	13.73 ± 0.05	22.0 ± 2.8	57	−12.2
	1037.617	2838.701	1.735790 ± 0.000017	13.73 ± 0.05	22.0 ± 2.8	32	−12.2

* The Doppler parameter has been fixed to improve the goodness-of-fit